Proceedings of the
Annual Stability Conference
Structural Stability Research Council
Louisville, Kentucky, April 1-4, 2025

Influence of residual stresses on the strength of horizontally curved steel I-girders

Aanandh Nandakumar[1], Lakshmi Subramanian[2]

Abstract
The ultimate load capacities of straight I-girders are notably affected by residual stresses, particularly in the inelastic buckling range where premature yielding of the flanges occurs. In contrast, horizontally curved I-girders experience substantial flange lateral bending due to their curvature, yet the impact of residual stresses on their load-carrying capacity remains inadequately understood. Past studies suggest that residual stresses have negligible effects on curved I-girders' load capacities but lack mechanistic explanations or consideration of varying residual stress patterns induced by different curving techniques. This paper explains the behavior of curved I-girders under various residual stress patterns documented in the literature for different curving methods. Specifically, the study evaluates the influence of assumed residual stresses on flange lateral bending and ultimate load capacity by comparing load-deformation responses and variations in flange stresses with those of straight I-girders by means of finite element simulations. The investigation encompasses a wide range of geometric parameters, such as cross-sectional aspect ratio and web slenderness, which are known to affect residual stress distributions.

1. Introduction

The manufacturing of I-sections typically involves either hot-rolling or welding, both of which introduce residual stresses into the I-sections. Hot-rolled I-sections develop residual stresses due to uneven cooling of flange tips and web-flange junctions, while welded I-sections experience residual stresses from uneven heating during the welding process. The impact of these residual stresses on the ultimate load capacities of straight I-girders has been well-documented based on various experimental and numerical studies. Specifically, I-girders with slenderness in the inelastic buckling portion of the design curves are highly sensitive to initial residual stresses, which lead to premature yielding of the flange tips. The influence of the magnitude and distribution of residual stresses on the capacities of straight I-girders can be understood by using finite element (FE) test simulations, where residual stresses are input as the initial stress condition. These initial conditions

[1] Research Scholar, Department of Civil Engineering, Indian Institute of Technology Madras, <aanandhkrish@gmail.com>
[2] Assistant Professor, Department of Civil Engineering, Indian Institute of Technology Madras, <lakshmipriya@iitm.ac.in>

are often based on the residual stress models from previous research, supported by experimental measurements. For example, Subramanian and White (2017) utilized models proposed by Galambos & Ketter (1959), Prawel et al. (1974), and ECCS (1976) to assess the impact of residual stresses on the lateral torsional buckling (LTB) capacity of straight I-girders.

The curving technique used in manufacturing horizontally curved girders can additionally alter the existing residual stresses from hot-rolling or welding. I-girders are typically either heat-curved or cold-curved. Heat-curving involves multiple passes of heating and cooling to achieve the desired curvature, while cold-curving uses a series of hydraulic presses. The changes in residual stresses due to the curving process have been documented by Brockenbrough & Ives (1970) and Gergess (2001). However, the influence of these residual stresses on the ultimate capacities of the curved I-girders has only been partially addressed in the experimental and analytical works by Shanmugam et al. (1995), Liew et al. (1995) and Davidson et al. (2000a&b). For instance, Liew et al. (1995) observed that the presence or absence of residual stresses does not influence the ultimate load capacities of curved girders across the entire beam strength curve, based on the analysis of a single hot-rolled cross-section. White et al. (2001) considered the effect of heat-curving on the residual stresses, and the changed residual stress pattern was subsequently used in their finite element (FE) models. Other numerical studies, such as those by Jung & White (2006), Issa-El-Khoury et al. (2014 & 2016), Frankl & Linzell (2020a&b), have often used residual stress models for straight girders in studying horizontally curved girders. Nonetheless, past research has not adequately explained the mechanistic influence of residual stresses on the load capacities of the curved girders, which are prone to large flange lateral bending stresses arising out of the curvature-induced torsion.

This paper systematically addresses the influence of residual stresses on the ultimate load-carrying capacities of the curved I-girders through FE test simulations, providing mechanistic explanations. The FE models in this study incorporate patterns used for straight girders and a simplified model proposed by the authors based on heat-curving. The scope of the study includes a wide range of geometric parameters, such as girder slenderness and curvature, considering webs of different slenderness classes and cross-sectional aspect ratios.

2. Methodology

This section details the finite element modeling conducted using ABAQUS (Simulia 2019), the material and geometric parameters that are considered, and the type of imperfections incorporated in the models.

2.1 Mesh discretization

The flanges and web are modeled using 4-noded S4R shell elements. Based on a mesh convergence study, twelve elements are used across the flange width, and forty elements are used along the web depth. The web element aspect ratios are kept close to one.

2.2 Material parameters

The homogeneous steel girders are modeled with a Young's modulus (E) of 200 GPa and a Poisson's ratio (ν) of 0.3. The yield strength, F_y, of the steel used, is 350 MPa. The constitutive model for the steel is shown in Fig. 1. A small tangent modulus of $E/1000$ is used for strain levels greater than the yield strain (ε_y) up to a strain level of $10\varepsilon_y$, beyond which a strain hardening

modulus of $E/50$ is considered. However, in practice, the strain levels in a horizontally curved girder are usually less than $10\varepsilon_y$.

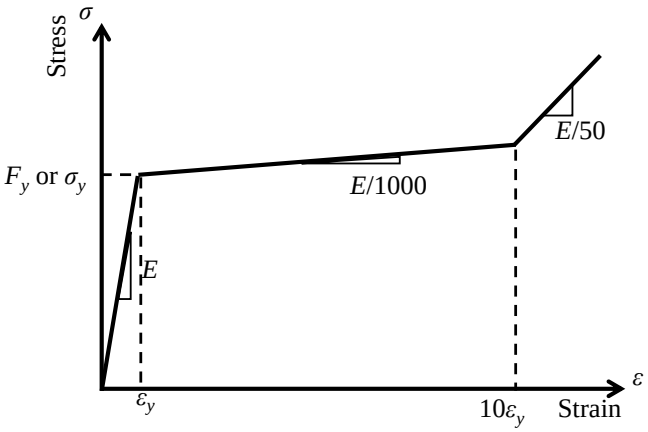

Figure 1: The constitutive model of the steel used in the FE models

2.3 Geometric parameters

The geometric parameters considered in the current study are limited to doubly symmetric cross-sections listed in Table 1. The web depth (D) considered for all the girders is 2m. Further, the web thickness is decided by the web slenderness that is studied. The current study looks at three different classes of the web (compact, noncompact, and slender) as per AASHTO (2020). The flange dimensions are determined based on the cross-sectional aspect ratio (D/b_f), while restricting the studies to compact flanges. For I-sections with compact webs, a D/b_f of one is considered in addition to the ratios of three and five, which are used for all three web classes. Combining the different parameters results in seven different cross-sections overall. In Table 1, t_w is the web thickness, b_f is the flange width, and t_f is the flange thickness.

The length of the girders is decided based on the girder slenderness parameter, λ_{LT}, which is defined by Eq. 1 for sections with compact webs and Eq. 2 for noncompact and slender web I-girders. Although the noncompact web girders (defined as per AASHTO (2020)) have capacities higher than the yield capacity M_y, for uniformity, the girder slenderness is defined based on the yield moment capacities. A wide range of girder slenderness is considered, as shown in Table 1, to understand the influence of residual stress in the plastic, inelastic, and elastic range of girder slenderness, as defined for straight girders. However, it should be noted that no such definitions are available for curved I-girders by any international standards.

$$\lambda_{LT} = \sqrt{\frac{M_p}{M_{cr}}} \tag{1}$$

$$\lambda_{LT} = \sqrt{\frac{M_y}{M_{cr}}} \tag{2}$$

where, M_p is the full plastic capacity of the I-section about the major axis, and M_{cr} is the elastic critical buckling moment capacity of straight I-girders subjected to uniform moments (defined by Timoshenko et al. (1962)).

The radius of curvature for the girders is defined using L_b/R, where the radius is determined based on the arc length of the girder (L_b). Additionally, some cases for equivalent straight girders ($L_b/R = 0$) are also included to illustrate the differences in the behavior of curved girders due to residual stresses. This work includes extreme L_b/R values of up to 0.20 since this work aims to establish the effect of residual stresses over the entire range of girder slenderness.

Table 1: The list of geometric parameters in doubly symmetric sections considered in the present study

Geometrical parameter	Values						
Girder (G)	1	2	3	4	5	6	7
Web slenderness (D/t_w)	60	60	60	120	120	200	200
Web classification as per AASHTO	Compact	Compact	Compact	Non compact	Non compact	Slender	Slender
Flange slenderness ($b_f/2t_f$)	8.9	8.3	5	8.3	5	8.33	5
Flange classification as per AASHTO	Compact	Compact	Compact	Compact	Compact	Compact	Compact
Cross-sectional aspect ratio (D/b_f)	1	3	5	3	5	3	5
Girder slenderness (λ_{LT})	0.2 to 2.0						
Curvature (L_b/R)	0 (Straight), 0.05, 0.10, 0.15 and 0.20						

2.4 Loading and boundary conditions

The girders are simply supported in flexure and torsion i.e., the girder ends are restrained from twisting and free to warp. They are subjected to a nearly uniform moment loading condition, as shown in Fig. 2.

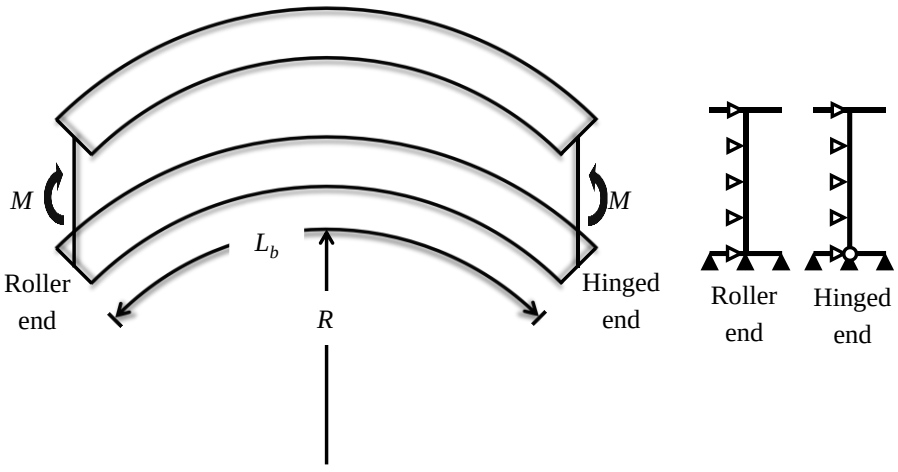

Figure 2: Loading and boundary conditions used in the FE models

In addition, Vlasov beam kinematics are applied at the girder ends to prevent cross-sectional distortion. The authors derive these end conditions for curved girders based on similar expressions available for straight girders in Kim (2010).

2.5 Residual Stresses and Initial Geometric Imperfections

In the present study, near-zero geometric imperfections (negligible flange sweep of $L_b/10000$) are used to isolate the impact of the residual stresses on girder capacities.

The typical patterns considered for straight girders from Galambos & Ketter (1959), Prawel et al. (1974), and ECCS (1976) for hot-rolled and welded I-section residual stresses are used in these studies. In addition, the girders are modeled with a residual stress distribution specific to heat-curved I-girders. This post-curving (heat) residual stress distribution is a simplified representation of the Gauss-point residual stresses given by White et al. (2001), based on the heat-curving procedure carried out by Brockenbrough & Ives (1970). Furthermore, all girders are modeled with no residual stresses to quantify the effect of each assumed residual stress distribution.

Fig. 3(a) shows the hot-rolled residual stress distribution as per ECCS (1976), while Fig. 3(b) corresponds to the distribution given by Galambos & Ketter (1959). The notation r is assumed to be 0.5 for I-sections with cross-sectional aspect ratios (D/b_f) less than one, and 0.3 for those greater than one. Positive regions indicate tensile residual stresses, and negative indicates compressive stresses. The notation g is defined based on Eq. 3:

$$g = \frac{A_f}{A_f + A_w} \tag{3}$$

where A_f is the area of the flange and A_w is the area of the web.

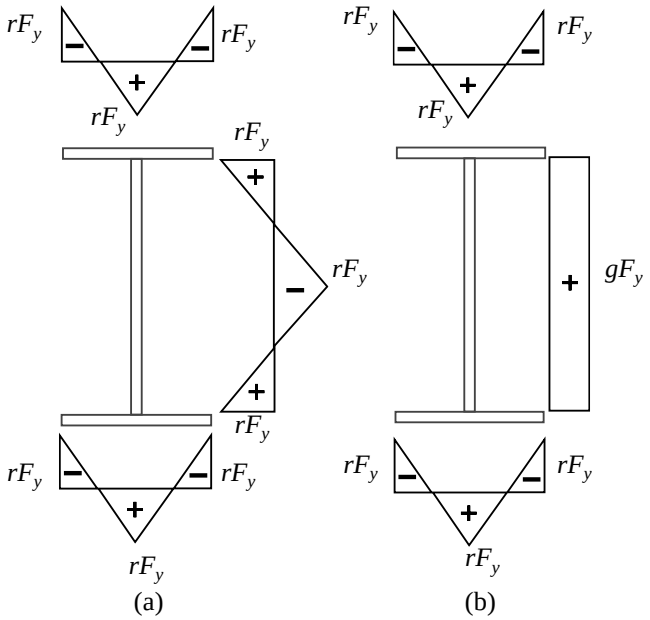

Figure 3: Residual stress distribution typical for straight hot-rolled I-sections given by (a) ECCS (1976) and (b) Galambos & Ketter (1959)

Figs. 4(a) and (b) correspond to the welded residual stress distribution given by Subramanian and White (2017) (based on Prawel et al. (1974)) and ECCS (1976), respectively. The notations c and F_c are as explained in Subramanian and White (2017), where F_c refers to the magnitude of the

compressive residual stress block, and *c* denotes the width of tensile residual stress blocks in the web and flange plates of the I-section.

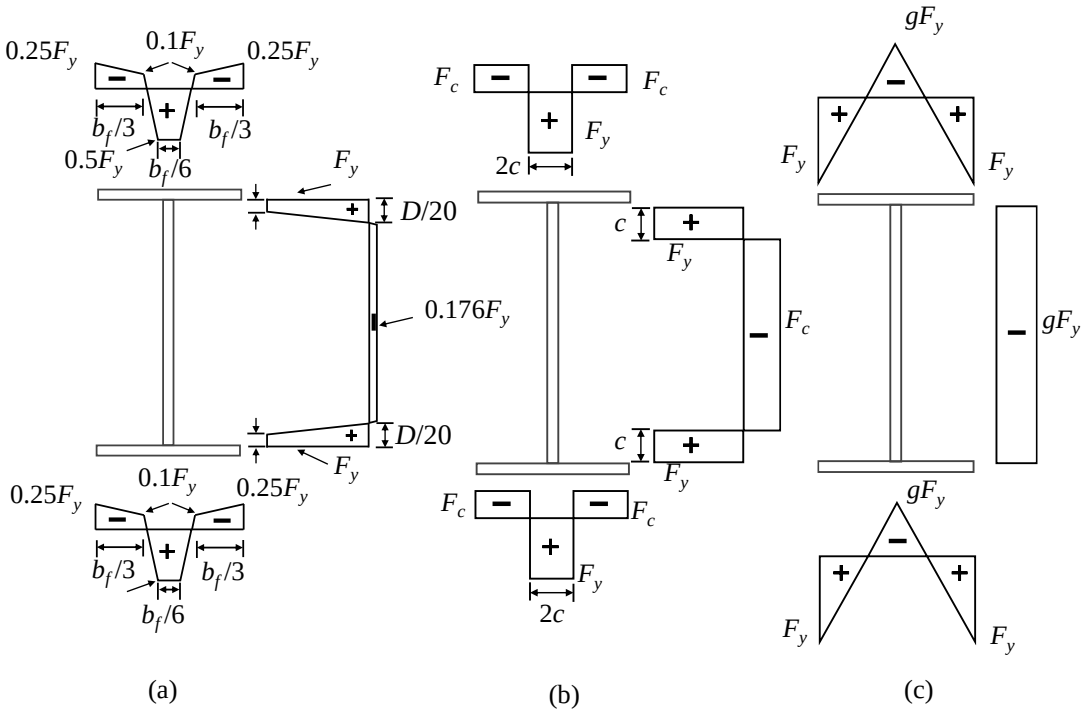

Figure 4: Residual stress distribution typical for straight welded I- sections given by (a) Subramanian and White (2017) and (b) ECCS (1976); (c) Simplified proposed model for residual stresses in heat-curved I-girders

Fig. 4(c) illustrates the simplified proposed residual stress model for heat-curved I-girders (Nandakumar and Subramanian 2025), wherein the flange tips experience tensile residual stresses of magnitude equaling the yield strength of the steel (F_y). Further, the explanations for the notations *r* and *g* are similar to the discussions provided for the hot-rolled residual stress model given by Galambos & Ketter (1959).

4. Results and Discussion

This section discusses the results obtained from the FE analysis of both straight and curved I-girders, comparing the key findings pertinent to each girder type.

4.1 Comparison of the girder responses

This section compares the response of the straight and curved girders based on the residual stresses assumed in the FE models. Furthermore, the load vs out-of-plane displacement profiles, strain profiles, and stress profiles are compared amongst girders of different curvatures.

4.1.1 Load-deflection characteristics

This section presents the load vs out-of-plane displacements measured at the midspan at the top web-flange junction. Figs. 5 and 6 show the differences in the load-displacement profiles among the three different classes of web considered in the present study (girders G3, G5, and G7) while keeping the cross-sectional aspect ratio (D/b_f) as five and girder slenderness (λ_{LT}) as 0.7 in all the cases.

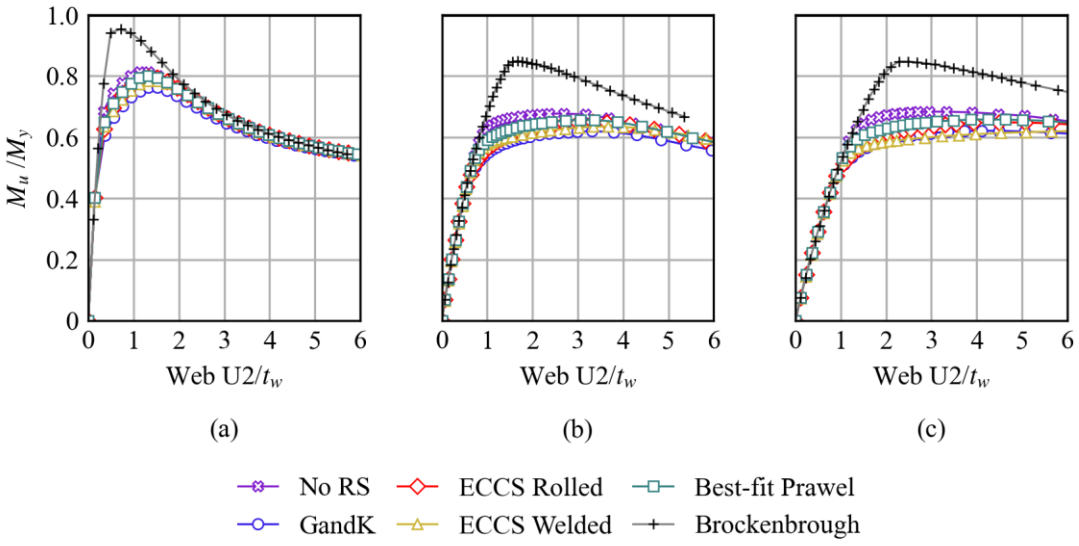

Figure 5: Load vs out-of-plane displacement profiles for girders with L_b/R = 0.05, λ_{LT} = 0.7; (a) G3, (b) G5, and (c) G7

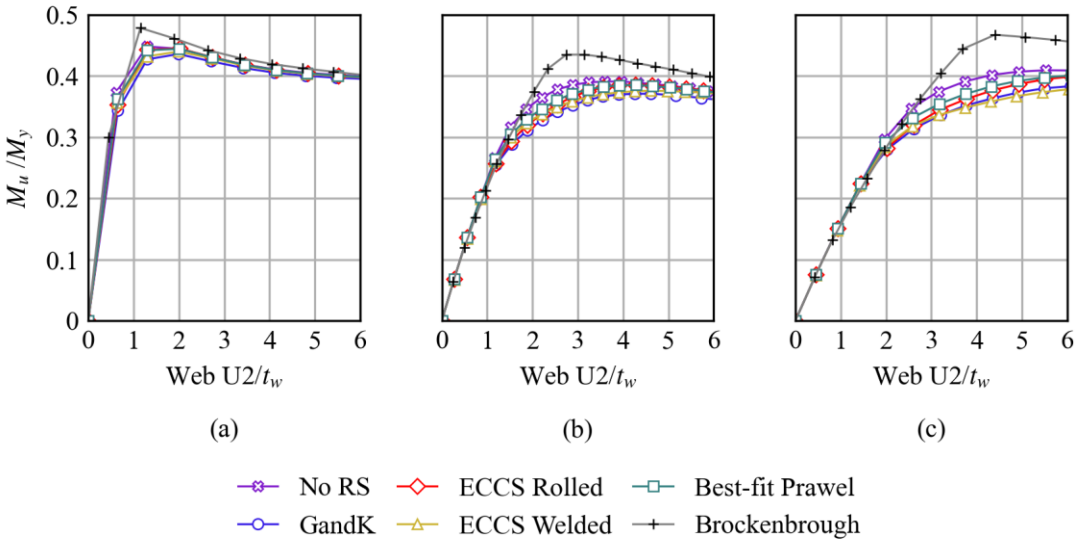

Figure 6: Load vs out-of-plane displacement profiles for girders with L_b/R = 0.20, λ_{LT} = 0.7; (a) G3, (b) G5, and (c) G7

The following may be gleaned from the results.

1. In all presented cases, the curved girder responses are stiffest when the residual stresses assumed are based on the proposed simplified model for heat-curved girders. The girders without residual stresses are relatively more flexible than those with heat-curved residual stresses that have tensile stresses at the flange tips.
2. The flexibility of girders increases with the magnitude and distribution of compressive residual stresses. Consequently, girders with post-welding residual stresses recommended by ECCS (1976) are the most flexible.

3. As expected, the flexibility of the girders is also governed by the web slenderness and the curvature, thereby making the girders with L_b/R of 0.05 and compact web stiffer than the girders with L_b/R of 0.20 and slender web.
4. Regardless of the initial residual stresses, the peak loads attained by all girders for a given curvature and web slenderness are not significantly different, with marginally larger peak capacities in the girders with heat-curved residual stresses.

Although the aforementioned observations pertain to a specific girder length, similar trends of load-displacement profiles are expected across various girder slenderness. However, a reduction in girder length leads to stiffer responses.

4.1.2 Strain and stress profiles

This section examines the mechanistic reasons for the insensitivity of curved girders to the initial residual stresses by studying longitudinal strains and stresses, and flange plastification.

Fig. 7 compares the levels of plastification observed across the flange widths for each of the assumed residual stress patterns for girder G1 by analyzing the von Mises stresses at the respective peak loads. The results presented pertain to wider-flanged sections with compact webs and a curvature of 0.20. The darker regions indicate portions of the girder that are yielded. Figs. 8 and 9 present the variation of flange longitudinal strains and stresses across the flange width, respectively for girder (G1) with compact web, cross-sectional aspect ratio (D/b_f) of one, and girder slenderness (λ_{LT}) of 0.7. The strains and stresses are normalized with the yield strain and yield stress. In addition, they compare the strain profiles of G1 with slenderness 0.2 and 1.2. Figure 1010 compares the strain levels of G1 girders for two different girder slenderness (λ_{LT}) of 0.2 and 1.2 to explain the effect of girder slenderness on the levels of flange lateral bending undergone by straight and curved girders. However, the interpretations from Figure 1010 can be extended to girders of any cross-sectional aspect ratio.

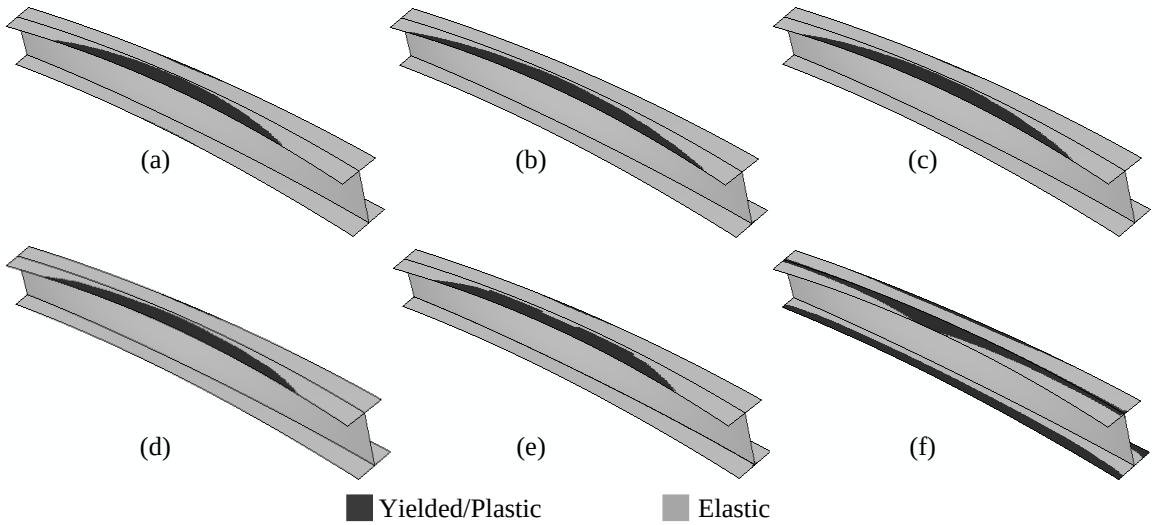

Figure 7: von Mises stress contours for G1 girder with L_b/R = 0.20, λ_{LT} = 0.7 having (a) No residual stress, and residual stresses based on (b) ECCS Rolled, (c) GandK, (d) Best-fit Prawel, (e) ECCS Welded and (f) Brockenbrough

The following may be gleaned from the results.

1. Fig. 7 indicates that the level of plastification across the compression flange width is similar, regardless of the initial residual stress condition. Further, the flanges exhibit greater plastification from the face of the compression flange that faces the center of curvature because the compressive stresses at these fibers arise from both direct stresses and the flange lateral bending stresses. In other words, the top flange in a curved I-girder is not uniformly compressed.
2. The curvature-induced flange lateral bending causes tensile stresses at the outer edge of the top flange, thereby establishing a stress gradient within the flange. This results in early yielding due to residual stresses in only one flange tip, rather than in both flange tips when the flange is in uniform compression.
3. The non-uniform yielding of the top flange facilitates greater load-sharing, mitigating the effects of the different residual stress patterns. Consequently, the strength is then governed by the overall instability of the member.

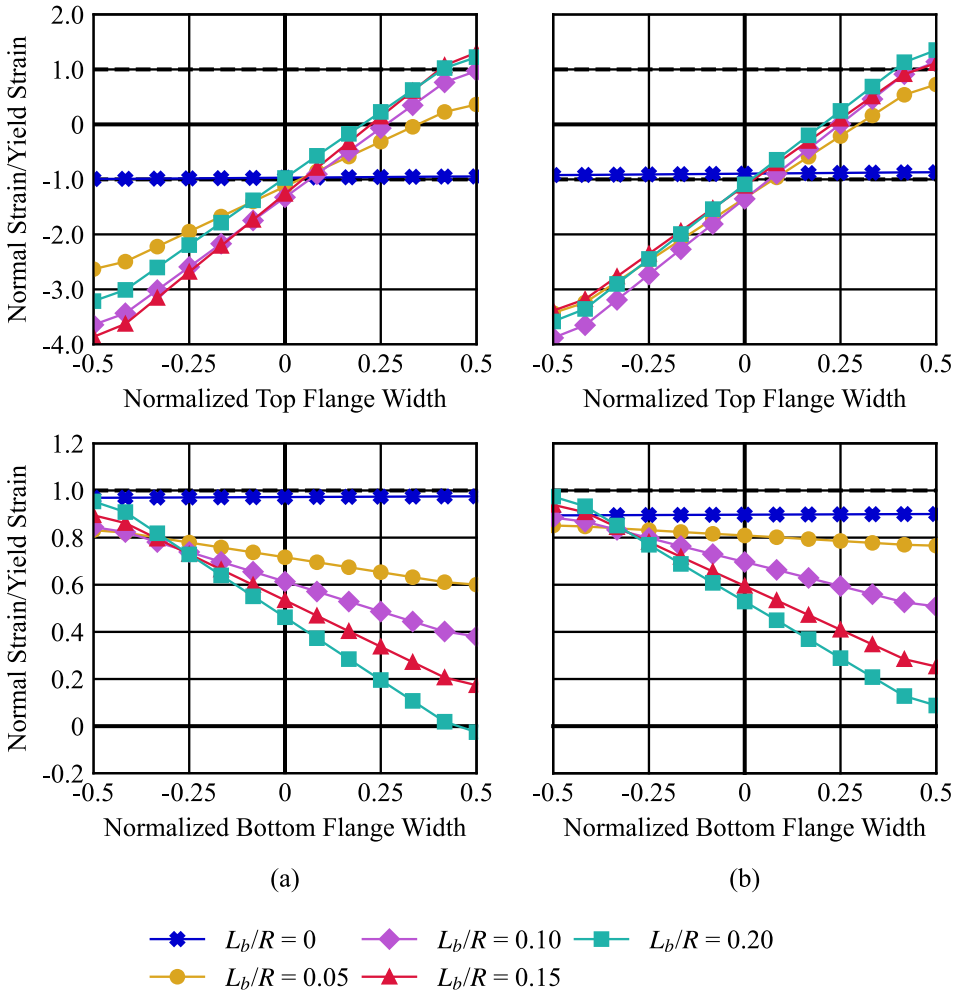

Figure 8: Normalized longitudinal (normal strains) for G1 girders with $\lambda_{LT} = 0.7$ and having (a) No residual stresses (b) ECCS (1976) welded residual stresses

4. According to Fig. 8, the strain levels reached by the inside edge (towards the center of

curvature) of the compression flange are nearly three to four times the yield strain of the material, while the outer edge (away from the center of curvature) barely reaches the yield strain, which is tensile. These high strain levels on one flange tip are observed for both initial residual stress conditions. Furthermore, these strain gradients correspond to the stress distribution observed in Fig. 9, where the stress profiles are similar for a given curvature, regardless of the initial residual stresses.

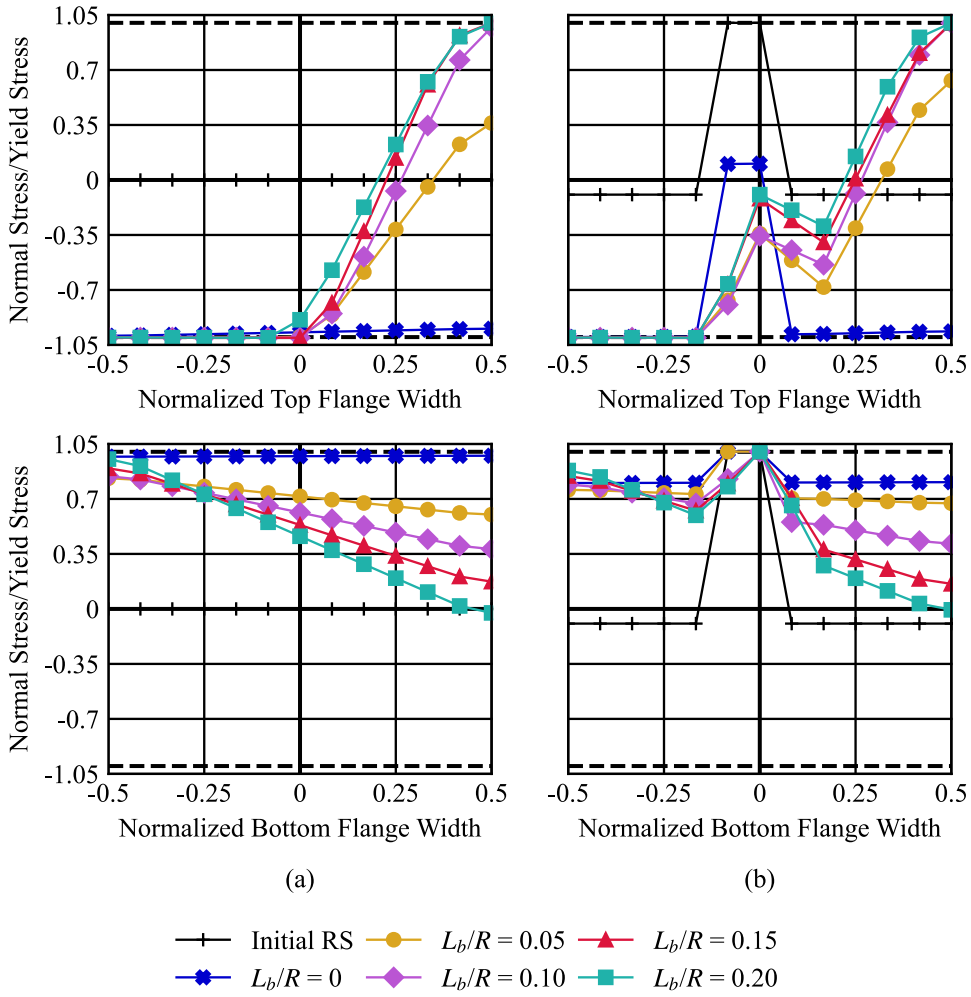

Figure 9: Normalized longitudinal (normal stresses) for G1 girders with $\lambda_{LT} = 0.7$ and having (a) No residual stresses (b) ECCS (1976) welded residual stresses

5. In contrast, all the fibers in a straight girder compression flange are strained uniformly, making straight girder strengths sensitive to the initial residual stress condition.
6. From Fig. 10, the strain levels attained by the inside edges of short-span curved girders can be as high as six to eight times the yield strain. Conversely, for longer straight girders, which primarily experience flange lateral bending, the strain levels are limited to the yield strain or less. Since the rectangular flange cross-sections possess sufficient reserve strength beyond the yield point, the compression flanges in curved girders can also endure higher strain levels beyond the yield strain, thereby neutralizing the effects of any initial residual stresses. However, the area of the web relative to the area of the flanges will make a difference in the

strain levels reached by the flanges. This beam-column behavior of the compression flange is effective up to the point where the overall stability of the girder is compromised.

7. Although a minor sensitivity to residual stresses is observed in both flanges of curved girders, their overall strength and stability are largely influenced by the stress levels reached by the compression flange. Further, as indicated by Fig. 910(b), there is a minor effect on the flange longitudinal stress profile based on the assumed residual stress. However, this effect is not adequate to cause significant differences in the girders' strengths.

The aforementioned points are valid for webs of any slenderness and cross-sectional aspect ratios.

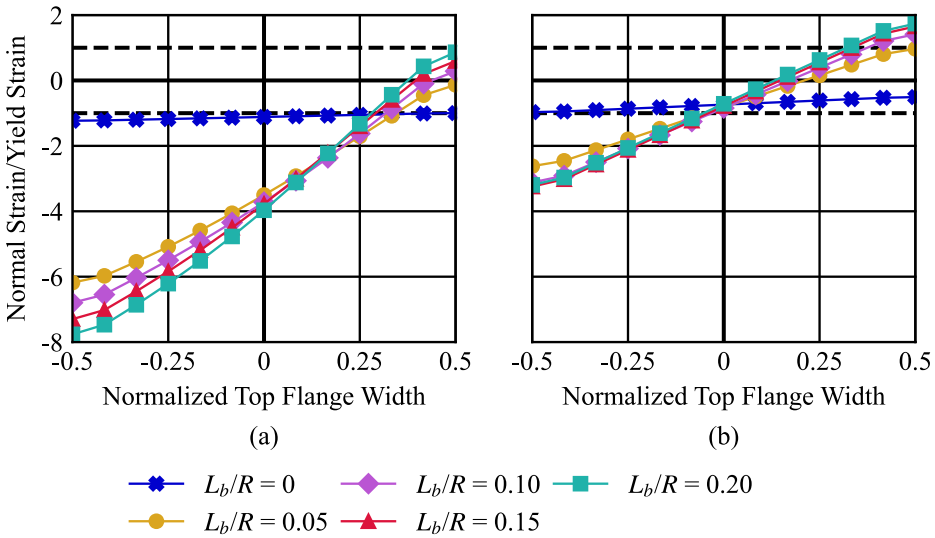

Figure 10: Normalized longitudinal (normal strains) for G1 girders, having no residual stresses and (a) λ_{LT} = 0.2 (b) λ_{LT} = 1.2

4.2 Girder strength curves

This section briefly examines the trends in the girder strength curves for all the curvatures, including straight girders, adopted in the current research.

4.2.1 Results for curved girders with compact webs

This section presents the results of the curved I-girders with compact webs. It is well-established that curved I-girders exhibit smaller capacities than their straight counterparts, attributable to the additional torsional shear stresses induced by curvature. Nonetheless, several additional observations on the behavior are addressed in the following discussions. Figs. 11 and 12 show the variation of the flexural capacities of curved I-girders (L_b/R values of 0.05 and 0.20) relative to the beam slenderness λ_{LT}, wherein Fig. 11 corresponds to G1 girders and Fig. 12 to G3 girders. In both figures, Brockenbrough refers to girders modeled with post-curving (heat) residual stresses, while No RS refers to girders with no residual stresses. Further, GandK refers to girders with residual stresses based on Galambos & Ketter (1959), and ECCS Rolled and ECCS Welded are based on ECCS (1976). Furthermore, Best-fit Prawel is based on residual stresses from Subramanian and White (2017). Fig. 13 compares the compression flange stress profiles of G1 (D/b_f = 1), and G3 (D/b_f = 5) curved girders modeled with post-curving (heat) residual stresses, and shows the variation in the flange plastification for different cross-sectional aspect ratio.

The following are gleaned from Figs. 11 - 13.

1. The flexural capacities of the curved I-girders are not affected by the magnitude and distribution of the assumed residual stresses; the difference in the capacities between girders with different residual stress patterns is less than 5%.
2. A girder modeled with an assumed residual stress pattern is of comparable strength to the one modeled without residual stress.

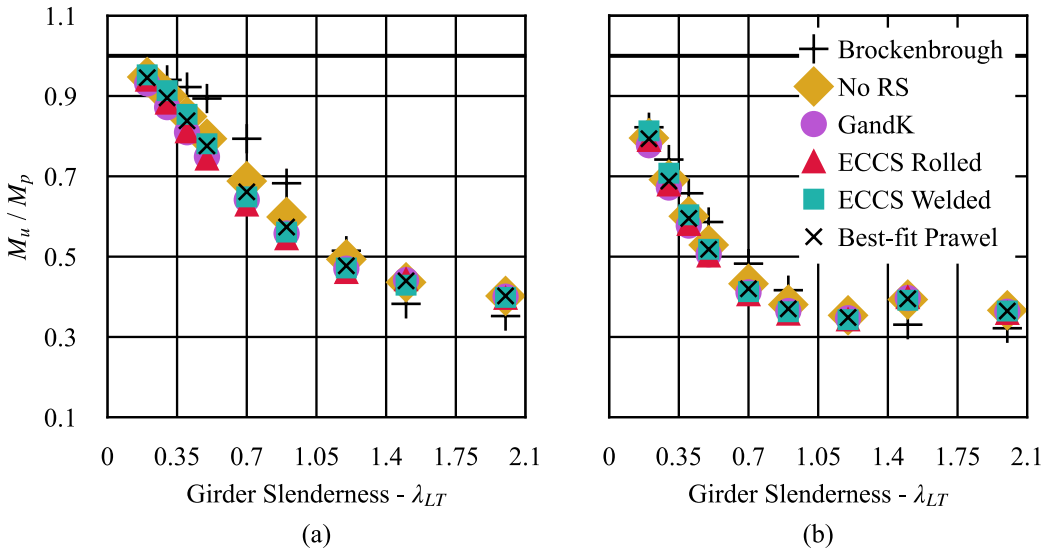

Figure 11: Beam strength curves for G1 girders with curvature of (a) L_b/R = 0.05 and (b) L_b/R = 0.20

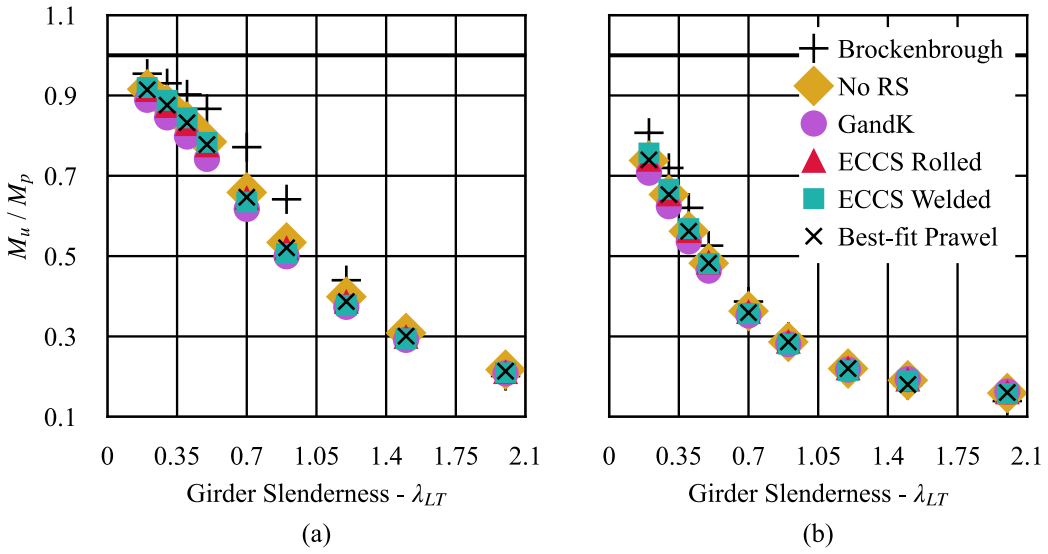

Figure 12: Beam strength curves for G3 girders with curvature of (a) L_b/R = 0.05 and (b) L_b/R = 0.20

3. The assumption of heat-curved residual stresses yields improved estimates of the girders' flexural strengths (G1 girders) within the inelastic range of the girder slenderness (λ_{LT} = 0.5 to 0.9) for a curvature (L_b/R) of 0.05. The maximum observed difference is 26% (compared to girders with ECCS (1976) welded residual stresses) and occurs at a girder slenderness of λ_{LT} =

0.7. However, with an increased curvature (L_b/R) of 0.20, the difference is reduced to 18%.

4. Curved girders modeled with post-welding or post-hot-rolling residual stress patterns, as stipulated by ECCS (1976), attain the smallest flexural capacity across various levels of girder slenderness. This trend is attributed to the constant compression stress block assumed in the flanges, which significantly reduces the effective flange width upon yielding of flange tips.
5. For heat-curved I-girders, the presence of tensile residual stresses within the compression flange enhances the flexural capacities of curved girders, irrespective of the curvature levels.
6. The flexural capacities of curved I-girders are also influenced by the cross-sectional aspect ratio (D/b_f), akin to straight girders. Fig. 12(b) demonstrates that larger curvature levels (L_b/R = 0.20) exacerbate stability issues in girders with relatively narrow flanges (D/b_f = 5), i.e., for G3 girders.
7. The benefits gained from tensile residual stresses in heat-curved girders with D/b_f = 1 (G1) is diminished in girders with D/b_f = 5 (G3). The capacity difference between girders with heat-curved and hot-rolled residual stresses at girder slenderness (λ_{LT}) of 0.7 (Galambos & Ketter, 1959) are 24% and 14% for L_b/R values of 0.05 and 0.20, respectively. This reduction is due to the smaller effective widths of flanges in narrow-flanged sections containing tensile residual stresses. In other words, the changes in the strengths come from the differences in the longitudinal stress profiles in the compression flanges of G1 and G3 girders at girder slenderness (λ_{LT}) of 0.7, as shown in Fig. 13.
8. It may be seen from Fig. 13, that for a given girder slenderness and curvature, wider flanges have larger compressive stresses than girders with narrow flanges. For instance, for a curvature of 0.10, nearly 60% of the flange width in G1 girders is in compression, while it is only 40% in G3 girders.

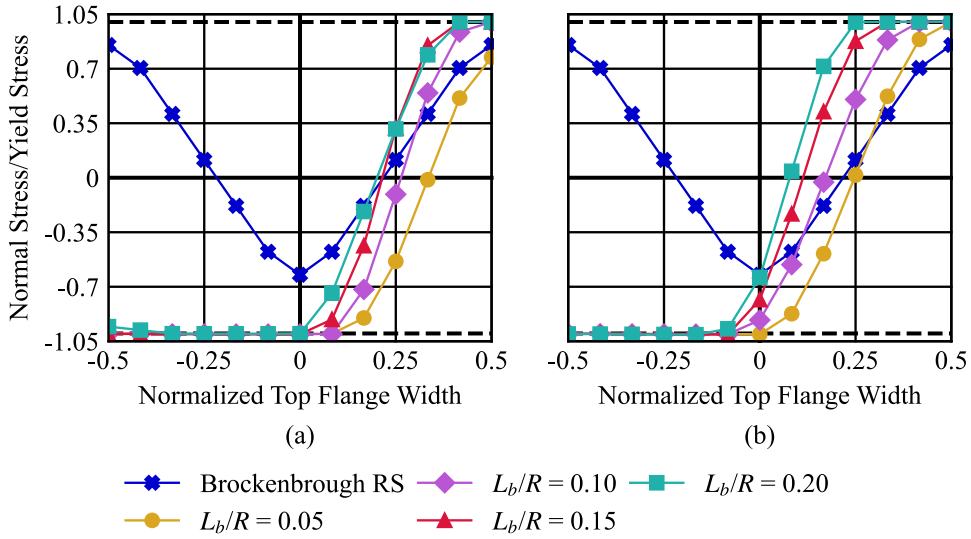

Figure 13: Comparison of compression flange stress profiles of G1 and G3 girders with λ_{LT} = 0.7

4.2.2 Results for curved girders with noncompact and slender webs

This section discusses the results of curved I-girders with noncompact and slender webs. While the previous discussions on compact webs generally apply to these other web classes, additional insights are provided here.

Figs. 14 and 15 show the results for noncompact and slender webs, respectively. The FE strengths are normalized by the cross-section's yield moment capacity (M_y). The presented results correspond to girders with a cross-sectional aspect ratio (D/b_f) of five (G5 and G7 girders). However, similar trends in the results are observed for the cross-sections with D/b_f of three.

The following are gleaned from the results.

1. The sensitivity to residual stresses is not evident in curved girders with noncompact and slender webs. As the curvature (L_b/R) increases to 0.20, the advantage gained from tensile residual stresses in flange tips of heat-curved girders becomes negligible. However, for mildly curved cases (L_b/R = 0.05), these stresses cause a difference between 15 -18% in the inelastic beam design range.

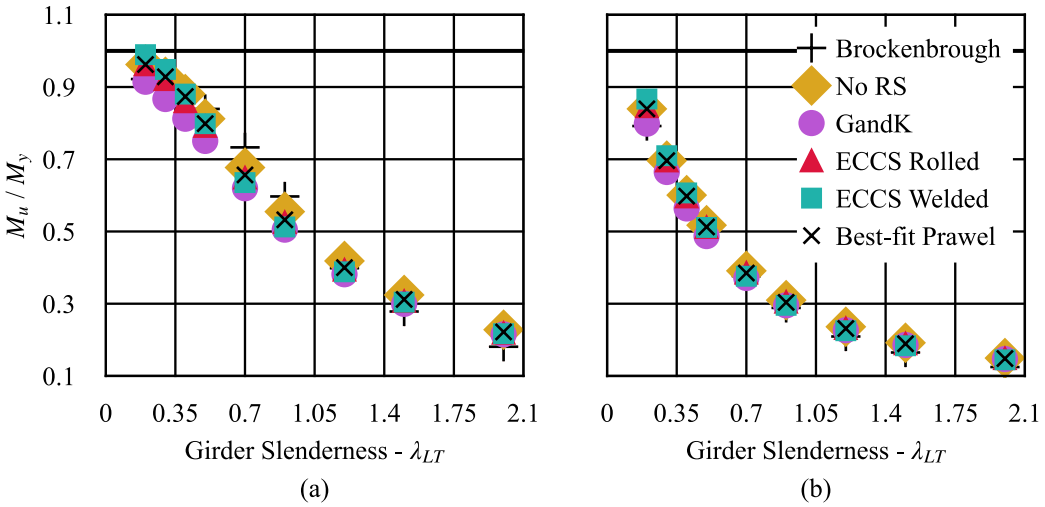

Figure 14: Beam strength curves for G5 girders having a curvature of (a) L_b/R = 0.05 and (b) L_b/R = 0.20

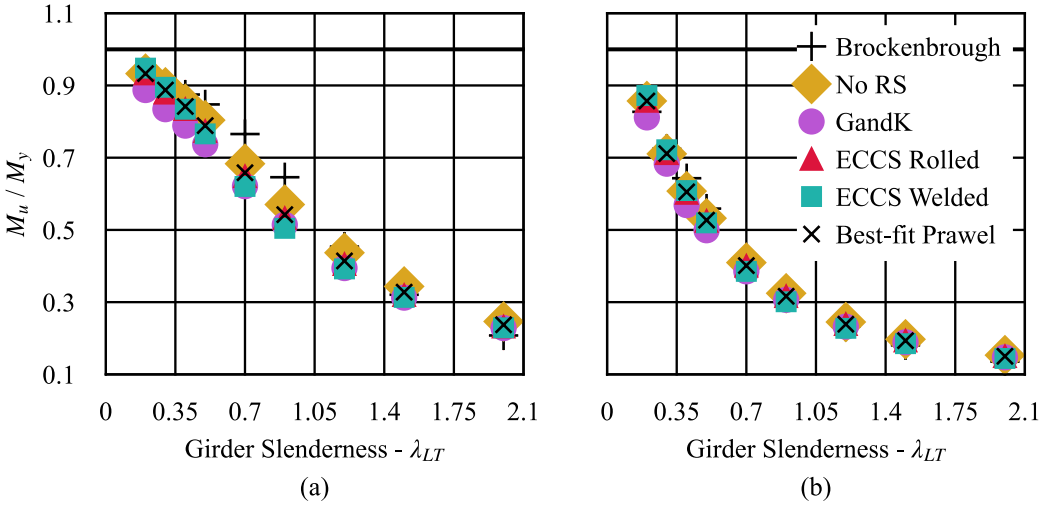

Figure 15: Beam strength curves for G7 girders having a curvature of (a) L_b/R = 0.05 and (b) L_b/R = 0.20

2. With an increase in curvature, the ability of the noncompact web girders to attain their respective yield moment capacities is reduced. The difference in the results between noncompact and slender web girders is not significantly different.

4.2.3 Comparison of strength curves for straight and curved girders of different curvatures
This section compares the capacities of straight and curved girders based on the assumed residual stress distributions.

Figs. 16 and 17 compare the flexural capacities of straight and curved I-girders under various residual stress conditions, including no residual stress, and hot-rolled and welded residual stresses specified by ECCS (1976). Specifically, Fig. 16 pertains to girders with compact webs and D/b_f of one (G1 girders), while Fig. 17 corresponds to girders with slender webs and D/b_f of five (G7 girders).

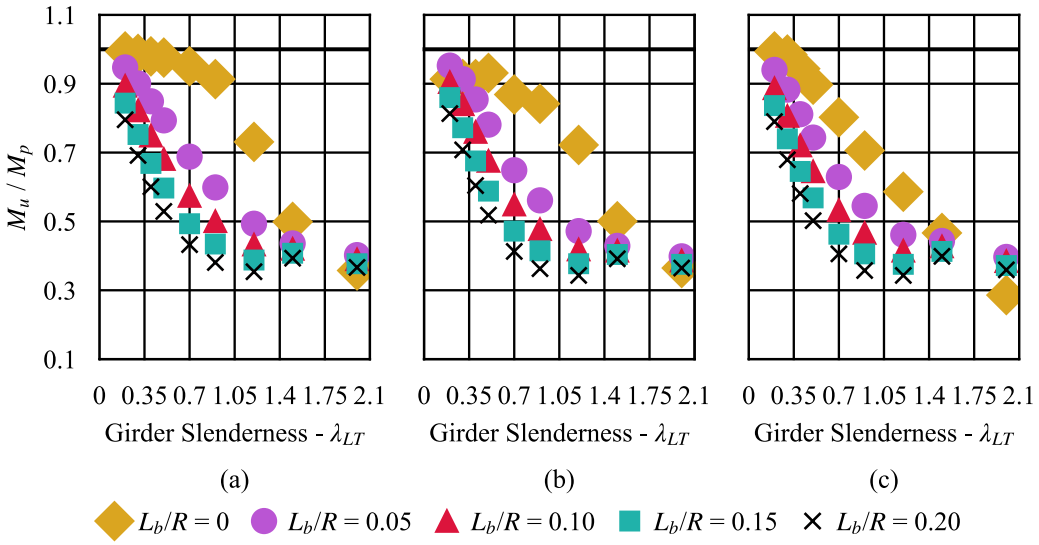

Figure 16: Comparison of capacities of G1 girders (straight and curved) with (a) No residual stresses, (b) ECCS (1976) welded and (c) ECCS (1976) hot-rolled residual stresses

The following may be inferred from the results.

1. In the plastic range of the girder strength curves, the flexural capacities of the straight girders modeled with no residual stresses reach their plastic moment capacity when the web is compact, while the slender web girders fall just short of their respective yield moment capacity ($0.95M_y$). However, the presence of curvature, which induces flange lateral bending, results in a reduction in the cross-sectional capacities. A similar reduction in capacities is also observed in girders with residual stresses.
2. The plateau lengths of straight girders with no residual stresses extend up to a girder slenderness of 0.5. However, no similar plateau region is observed even for the mildly curved girders ($L_b/R = 0.05$), showing that even girders with small curvature undergo sufficient flange lateral bending to experience a drop in their overall flexural capacities.
3. Residual stresses influence the flexural capacities of straight girders in the inelastic buckling region. For instance, comparing girders with no residual stresses to those with ECCS (1976) welded residual stresses, the difference in capacities is approximately 8 to 10% in the inelastic range of the girder slenderness ($\lambda_{LT} = 0.7$) when the web is compact, while the difference is close to 27% when the web is slender.
4. Typically, the girder strength curves are convex in nature. However, with increasing curvature,

the convexity of the girder strength curves reduces, becoming increasingly concave for girders with larger curvature. Such trends are observed across all residual stress conditions, consistent with the findings reported by Liew et al. (1995).

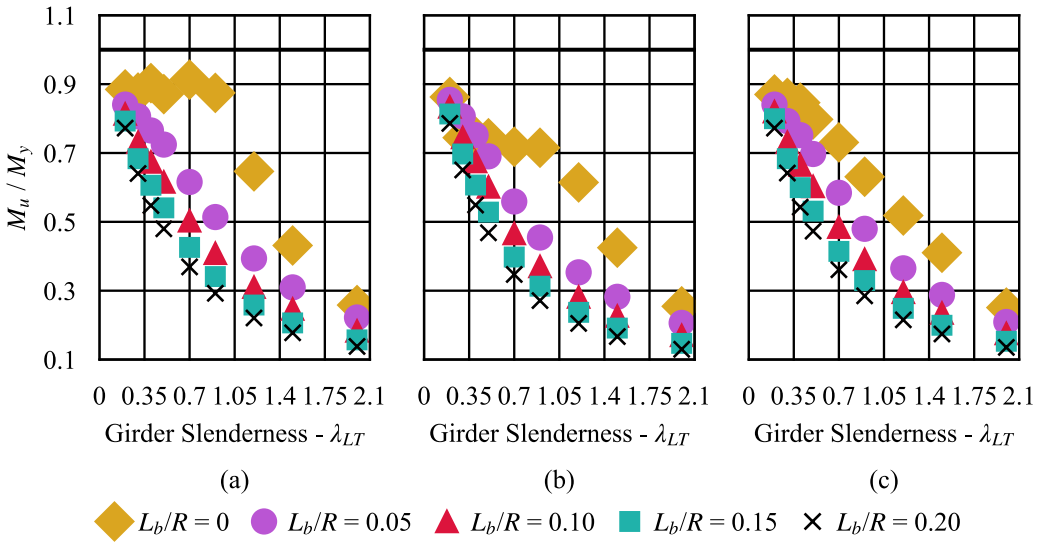

Figure 17: Comparison of capacities of G7 girders (straight and curved) with (a) No residual stresses, (b) ECCS (1976) welded and (c) ECCS (1976) hot-rolled residual stresses

5. Conclusions

This paper examines the influence of residual stress modeling on the flexural strengths of curved I-girders by considering girders with compact, noncompact, and slender webs. The following conclusions are drawn from the current study.

1. The influence of residual stresses on the flexural capacities of horizontally curved I-girders is negligible. The variation in flexural capacity between girders modeled with different residual stress distributions from straight girders is less than 5%, indicating that residual stresses do not significantly affect the flexural performance of these girders.
2. The use of a simplified residual stress distribution for heat-curved girders results in an increase in flexural capacities for girders with webs of any slenderness. This increase is attributed to the stress gradient induced by flange lateral bending, which creates tensile residual stresses in both flanges. The maximum increase, up to 25%, is observed in the inelastic region of the beam-strength curves for girders with compact webs and a cross-sectional aspect ratio of one.
3. Curvature results in a nearly linear strain variation across both flanges, causing their behavior to resemble those of a beam-column of a rectangular cross-section. Consequently, the strain gradients in the compression flange in the ultimate condition cause similar stress distribution between girders imposed with different initial residual stress patterns.
4. Even mildly curved girders do not exhibit a clearly defined plateau region in the flexural strength curve, unlike their straight girder counterparts due to flange lateral bending. This suggests that a modified approach may be required for the design curve of curved girders.

Considering the minimal impact of residual stress patterns on the flexural capacities of curved I-girders, yet recognizing their effect on the load-deflection response, it is reasonable to apply

residual stress patterns typically used for straight girders when modeling curved girders. However, the authors recommend modeling curved I-girders with only initial geometric imperfections and excluding residual stresses, as the actual heat-curved residual stresses result in higher capacities and a stiffer response. Assuming alternative residual stress patterns may lead to overly conservative estimates of girder behavior.

Acknowledgments
The current work is funded by the Science and Engineering Research Board, India and it does not have any conflict of interest.

References

AASHTO. (2020). *AASHTO LRFD Bridge Design Specifications, 9th edition,*. American Association of State Highway and Transportation Officials, Washington, DC.

Brockenbrough, R. L., and Ives, K. S. (1970). "Experimental Stresses and Strains from Heat Curving." *Journal of the Structural Division*, 96 (7) 1305–1331.

Davidson, J. S.; Ballance, S. R.; Yoo, C. H. (2000). "Effects of Longitudinal Stiffeners on Curved I-Girder Webs." *Journal of Bridge Engineering*, 5 (2) 171–178.

Davidson, James S.; Ballance, Scott R; Yoo, C. H. (2000). "Behaviour of Curved I-Girder Webs Subjected to Combined Bending and Shear." *Journal of Bridge Engineering*, 5 (2) 165–170.

Davidson, J. S., Ballance, S. R., and Yoo, C. H. (1999). "Finite Displacement Behavior of Curved I-Girder Webs Subjected to Bending." *Journal of Bridge Engineering*, 4 (3) 213–220.

ECCS. (1976). *Manual on Stability of Steel Structures*. *European Convention for Constructional Steelwork, 2nd edition*. Liege, Belgium.

Frankl, B. A., and Linzell, D. (2020a). "Validation of Modified Shear-buckling Coefficients for Horizontally Curved Steel Plate Girders." *Journal of Constructional Steel Research*, 168 1–9.

Frankl, B. A., and Linzell, D. G. (2020b). "Shear-Buckling Coefficients for Slender, Horizontally Curved Plates." *Journal of Structural Engineering*, 146 (3) 1–6.

Galambos, T. V., and Ketter, R. L. (1959). "Proceedings of the American Society of Civil Engineers." *Journal of Engineering Mechanics Division*, 85 (2) 135–152.

Gergess, A. N. (2001). "Cold Bending and Heat Curving of Structural Steel I-Girders." Doctoral dissertation, Department of Civil and Environmental Engineering, University of South Florida, Tampa, FL.

Issa-El-Khoury, G., Linzell, D. G., and Geschwindner, L. F. (2014). "Computational Studies of Horizontally Curved, Longitudinally Stiffened, Plate Girder Webs in Flexure." *Journal of Constructional Steel Research*, 93 97–106.

Issa-El-Khoury, G., Linzell, D. G., and Geschwindner, L. F. (2016). "Flexure-Shear Interaction Influence on Curved, Plate Girder Web Longitudinal Stiffener Placement." *Journal of Constructional Steel Research*, 120 25–32.

Jung, S. K., and White, D. W. (2006). "Shear Strength of Horizontally Curved Steel I-Girders - Finite Element Analysis Studies." *Journal of Constructional Steel Research*, 62 (4) 329–342.

Kim, Y. D. (2010). "Behavior and design of metal building frames using general prismatic and web-tapered steel I-section members." Doctoral dissertation, Georgia Institute of Technology, Atlanta, GA.

Nandakumar, A., and Subramanian, L. (2025). "Influence of Heat-Curving on the Flexural Capacity of Horizontally-Curved Steel I-Beams." *Recent Developments in Structural Engineering, Volume 2*, 405–411.

Prawel, S. P., Morrell, M. L., and Lee, G. C. (1974). "Bending and Buckling Strength of Tapered Structural Members." *Welding Research Supplement*, 53 (2) 75–84.

Richard Liew, J. Y., Thevendran, V., Shanmugam, N. E., and Tan, L. O. (1995). "Behaviour and Design of Horizontally Curved Steel Beams." *Journal of Constructional Steel Research*, 32 (1) 37–67.

Shanmugam, N. E., Thevendran, V., Liew, J. Y. R., and Tan, L. O. (1995). "Experimental Study on Steel Beams Curved in Plan." *Journal of Structural Engineering*, 121 (2) 249–259.

Simulia. (2019). *ABAQUS/Standard Version 6.19*. Simulia, Inc., Providence, RI.

Subramanian, L., and White, D. W. (2017). "Resolving the disconnects between lateral torsional buckling experimental tests, test simulations and design strength equations." *Journal of Constructional Steel Research*, 128 321–334.

Timoshenko, S. P., Gere, J. M., and Prager, W. (1962). *Theory of Elastic Stability, Second Edition*. McGraw-Hill

book Company, Inc.
White, D. W., Zureick, A. H., Phoawanich, N., and Jung, S. K. (2001). *Development of unified equations for design of curved and straight steel bridge I-girders*. Final Report to AISI, PSI, Inc. and FHWA.